

## CHAPTER 7 RADIO NOISE

### 7.1 SYSTEM NOISE TEMPERATURE

#### 7.1.1 Basic Concepts of Electrical Noise

Electrical noise is developed in resistors or conductors, due to the random motions of electrons. The available noise power  $p$  at the terminals of a resistor in a one Hz bandwidth at radio frequencies is independent of the value of the resistance and frequency and is given by

$$p = kT \quad \text{W/Hz} \quad (7.1)$$

where  $k$  is Boltzmann's constant ( $1.381 \times 10^{-23}$  J/K) and  $T$  is temperature in kelvins (K). The noise power  $P$  in a bandwidth  $B$  in the radio frequency range is therefore given by

$$P = kTB \quad \text{W} \quad (7.2)$$

with  $B$  in Hz. The standard reference value,  $T_0 = 290$  K, is normally used for  $T$  in noise power calculations.

If a receiver or amplifier has a resistive input impedance, the noise power at the output terminals of the receiver will be

$$P_{out} = gkT_0B + P_i \quad \text{W} \quad (7.3)$$

where  $g$  is the power gain of the amplifier and  $P_i$  is noise which is generated internally within the amplifier. The noise performance of an amplifier can be measured by use of a noise figure  $F$  where  $F$  is defined by the relation

$$F = P_{out} / (gP_{in}) \quad (7.4)$$

with the subscripts representing output and input and with  $P_{in} = kT_0B$ . Alternatively, a noise temperature  $T_R$  can be used to describe the noise performance of the receiver such that

$$P_{out} = gk(T_0 + T_R)B \quad \text{W} \quad (7.5)$$

Making use of Eqs. 7.3- 7.5, it can be established that

$$F = 1 + T_R/T_o \quad (7.6)$$

and

$$T_R = T_o (F - 1) \quad K \quad (7.7)$$

An advantage of using  $T_R$  as a measure of the noise introduced by a receiver is that it refers to the input terminals of the receiver and is additive with respect to temperatures representing other noise sources that may be applied to the receiver input terminals, as in Eq. (7.5).

Consider next a resistive or dissipative attenuator at the temperature  $T_o$ . In many applications, one simply considers the power output of the attenuator to be the input power-- times the power "gain"  $g_a$  of the attenuator so that  $P_{out} = P_{in} g_a$ . It is convenient when working with noise to use a noise temperature in place of noise power itself. Following that practice in this case

$$T_{out} = T_{in} g_a \quad K \quad (7.8)$$

A resistive attenuator-- , however, does more than attenuate. It adds noise as well, and it is advantageous to refer this noise to the input terminals of the attenuator in the same way that noise is referred to the input terminals of an amplifier or receiver. To carry out this procedure, it is necessary to determine the input temperature of an attenuator such that the temperature accounts for the noise generated by the attenuator and is consistent with Eq. (7.8). The advantage is, as with amplifiers, that this noise temperature is additive with respect to noise temperatures representing other sources of noise that may be applied to the input of the attenuator. Then one can use Eq. (7.8) for an attenuator with  $T_{in}$  representing the sum of the attenuator input noise temperature and a temperature representing all other noise sources, if any, that may be present. (Fig. 7.1). It develops that for an attenuator by itself

$$T_{in} = (1 - g_a) T_o \quad K \quad (7.9)$$

and

$$T_{\text{out}} = (1 - g_a) T_0 \quad \text{K} \quad (7.10)$$

with  $l_a = 1 / g_a$ . If an antenna which introduces noise corresponding to the temperature  $T_A$  is connected to the input terminals of the attenuator then

$$T_{\text{in}} = T_A + (l_a - 1) T_0 \quad \text{K} \quad (7.11)$$

and

$$T_{\text{out}} = T_A g_a + (1 - g_a) T_0 \quad \text{K} \quad (7.12)$$

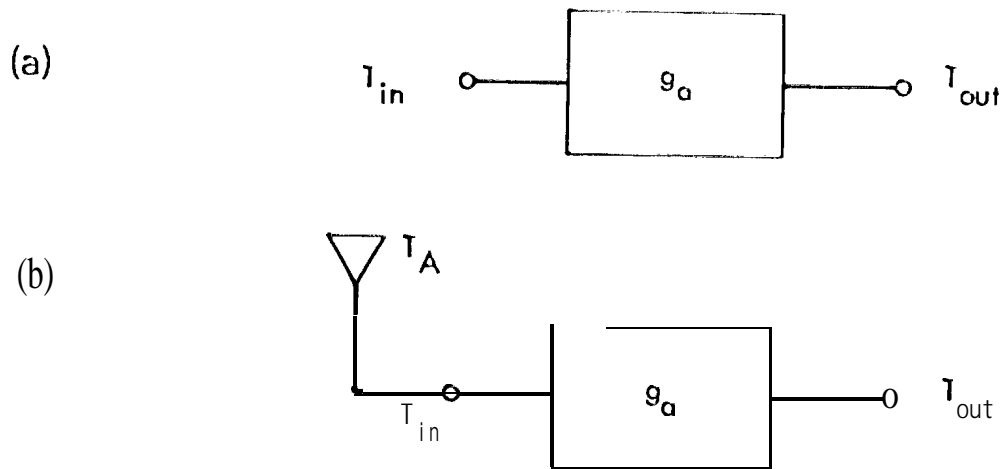


Figure 7.1. Concept of noise temperature of attenuator. For both situations  $T_{\text{out}} = T_{\text{in}} g_a$ . In Fig. (7. 1a), no input is connected to the attenuator and  $T_{\text{in}} = (l_a - 1) T_0$ . In Fig. (7. 1b),  $T_{\text{in}} = T_A + (l_a - 1) T_0$ , where  $T_A$  is the antenna noise temperature.

One additional basic relation is needed in order to define system noise temperature. Consider a system consisting of two separate parts connected in series as in Fig. 7.2.

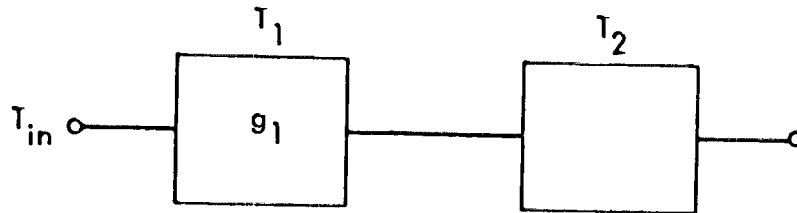


Figure 7.2. System of two parts connected in series and having temperatures of  $T_1$  and  $T_2$ .

It develops that

$$T_{in} = T_1 + T_2/g_1 \quad (7.13)$$

If  $g_1$  is the gain of an amplifier and is much greater than unity,  $T_1$  plays a greater role in determining  $T_{in}$  than  $T_2$ . Each of the two parts of the system may be an amplifier, attenuator, or combination of these. The concept illustrated by Eq. (7.13) can be extended to additional stages. For example, for a system of three parts,  $T_{in} = T_1 + T_2/g_1 + T_3/g_1g_2$ .

### 7.1.2 System Noise Temperature

Following Kraus (1986), system noise temperature  $T_{sys}$  is defined in Fig. 7.3, suggesting a telecommunication receiving system including an antenna having a noise temperature of  $T_A$ , a

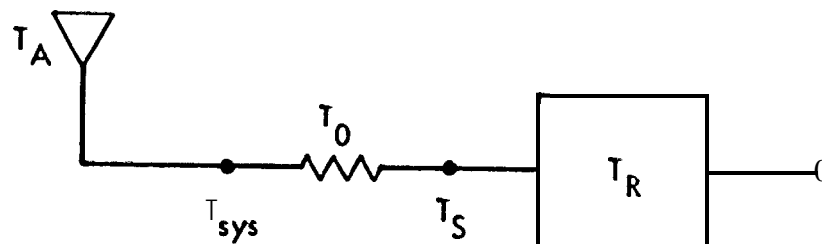


Figure 7.3. Locations where  $T_{sys}$  and  $T_s$  are defined.

dissipative transmission line which acts as an attenuator at a temperature of  $T_a = T_0$ , and a receiver having a noise temperature of  $T_R$ .  $T_{sys}$  is defined as the temperature at the antenna terminals and is given by

$$T_{sys} = T_A + (l_a - 1) T_0 + l_a T_R \quad K \quad (7.14)$$

Noise introduced by the antenna is accounted for by  $T_A$ . Then follows a term representing the input temperature of an attenuator at a physical temperature of  $T_0$  [corresponding to  $T_1$  of Eq.(7.13)], Finally,  $l_a T_R$  corresponds to  $T_2/g_1$  of Eq.(7.13) as  $l_a = 1/g_a$ .

Some analyses of telecommunication links make use of  $T_s$ , defined as at the receiver terminals, rather than  $T_{sys}$ . It is simple to convert from  $T_{sys}$  to  $T_s$  by using

$$T_s = T_{sys} g_a \quad K \quad (7.15)$$

resulting in

$$T_s = T_A g_a + (1 - g_a) T_0 + T_R \quad K \quad (7.16)$$

Either  $T_{sys}$  or  $T_s$  can be used if carrier and noise powers are defined at the same location, either antenna or receiver terminals. Noise power  $X$  at the antenna terminals is given by

$$X = k T_{sys} B \quad W \quad (7.17)$$

and at the receiver terminals by

$$X = k T_s B \quad W \quad (7.18)$$

Note that if  $g_a = l_a = 1$ , corresponding to zero attenuation between the antenna and receiver

$$T_{sys} = T_s = T_A + T_R \quad (7.19)$$

The effective noise temperature of the antenna  $T_A$  is not its physical temperature but accounts for all the noise, including sky noise and noise of terrestrial origin, that appears at the output terminals of the antenna. The term sky noise includes noise emitted by the constituents of the Earth's atmosphere, namely gases, hydrometers, and any other matter such as dust. It also includes extraterrestrial noise emitted by the Sun, Moon, planets, and universe, including the 2.7 K component which fills space. Terrestrial noise may be picked up by the side lobes or as a result of antenna spillover and blockage, in the case of the earth-station antenna. The main lobe, however, of a satellite--borne antenna is usually pointed at the Earth and receives noise of terrestrial origin. Interfering signals can also be considered to constitute noise which contributes to  $T_A$ .

The system noise temperature can be decreased by placing a preamplifier at the antenna terminals. In that case, for a system otherwise the same as that of Fig. 7.3,

$$T_{\text{Sys}} = T_A + T_{\text{pre}} + \frac{(l_a - 1)T_o + l_a T_R}{g_{\text{pre}}} \quad (7.20)$$

For this procedure to be most effective, the noise temperature of the preamplifier,  $T_{\text{pre}}$ , must be low and its gain,  $g_{\text{pre}}$ , should be high. The contributions to  $T_A$  are considered in the following section.

## 7.2 ATMOSPHERIC CONTRIBUTIONS TO NOISE TEMPERATURE

The principal types of naturally occurring radio noise, generated externally to the receivers of telecommunication systems, are the noise of lightning discharges (commonly referred to as atmospheric noise), cosmic noise, thermal radiation from the atmosphere and nearby terrain and objects, and noise from the Sun, Moon, and distant planets. Noise from lightning predominates for frequencies below about 20 MHz, and cosmic noise tends to be most important between about 20 and 1000 MHz. Above 1000 MHz, atmospheric thermal noise tends to predominate, when the antenna points into space and not towards the Sun or other discrete source. Noise from

lightning occurs mainly at frequencies below the range of this handbook and cosmic noise is considered in Sec. 7.3. Attention is directed in this section to atmospheric thermal noise.

A basic relation concerning noise applies to the noise temperature  $T_b$  recorded when observing a noise source, represented by a temperature  $T_s$ , through an absorbing region. The relation for the zenith is

$$T_b = T_s e^{-\tau_\infty} + \int_0^m T(h) \alpha(h) e^{-\tau} dh \quad (7.21)$$

with

$$\tau_\infty = \int_0^\infty a(h) dh$$

and

$$\tau = \int_0^h a(h) dh$$

with  $a(h)$  the absorption coefficient expressed as a function of height  $h$  (Waters, 1976). When  $T(h)$  is a constant, a change of the variable of integration made by noting that  $\alpha(h) dh$  equals  $d\tau$  allows carrying out the integration and obtaining the simpler form (with  $\tau = \tau_\infty$ )

$$T_b = T_s e^{-\tau} + T_i (1 - e^{-\tau}) \quad (7.22)$$

The first term of Eq. (7.22) shows that the noise source beyond the absorbing region is attenuated by a factor of  $e^{-\tau}$ . The second term represents atmospheric thermal noise which may be generated whether there is a noise source  $T_s$  beyond the absorbing region or not. If  $\tau$  is zero, corresponding to no absorption, the second term is zero. If attenuation due to scattering occurs as well as absorption, Eq. (7.22) may need to be modified such that  $\alpha(h)$  represents absorption only. However, Eq. (7.22) may still be used as it is, with  $\alpha(h)$  representing extinction even when there is scattering, if an appropriate, effective temperature  $T_i$  can be determined. In this case,  $T_i$  will be less than the actual physical temperature of the absorbing region.

One procedure for determining  $T_i$  involves alternately pointing at the Sun and away from the Sun, The difference in the two values of  $T_b$  give  $T_s e^{-\tau}$  which allows determining  $T_i(1 - e^{-\tau})$  also. By recording  $T_b$  when pointing at the Sun with no obvious absorbing region present (no clouds or precipitation) and correcting for the small absorption due to gases, one can then determine  $T_s$  itself for the Sun. Knowing  $T_s$  allows determining  $e^{-\tau}$ . Finally, as all the other quantities of Eq. (7.22) are known by now,  $T_i$  can be determined as well.

Extraterrestrial noise corresponding to a noise temperature of 2.7 K is always present and this small value can be accounted for or ignored, in the latter case and in the absence of any other known source resulting in

$$T_b = T_i(1 - e^{-\tau}) \quad (7.23)$$

The value of the effective temperature  $T_i$  will be different at different times and locations, but taking it as 280 K appears to give generally good results in temperate regions. Wulfsberg and Altshuler (1972) found that 284 K was a suitable value for Hawaii. In other cases, where scattering was thought to be significant, lower temperatures such as 273 or 260 K have been used.

Figure 7.4 shows the estimated ratio of the extinction (total attenuation) constant to the absorption constant for a 12 mm/h rain model and for a cloud model, According to this figure, scattering is not important for clouds for frequencies below 50 GHz but is significant for rain of this intensity above about 5 GHz. Figure 7.5 shows a plot of Eq. (7.23) for  $T_i = 280$  K and also the relation  $T_b = 60 \text{ dB}^*$

For low-noise systems, the decrease in signal-to-noise ratio  $C/X$  due to noise is larger than the accompanying decrease due to signal attenuation, for attenuation up to about 10 dB. This condition is illustrated by Fig. 7.6 which is based upon Eq. (7.23) with  $T_i = 280$  K. To understand the basis for Fig. 7.6, consider



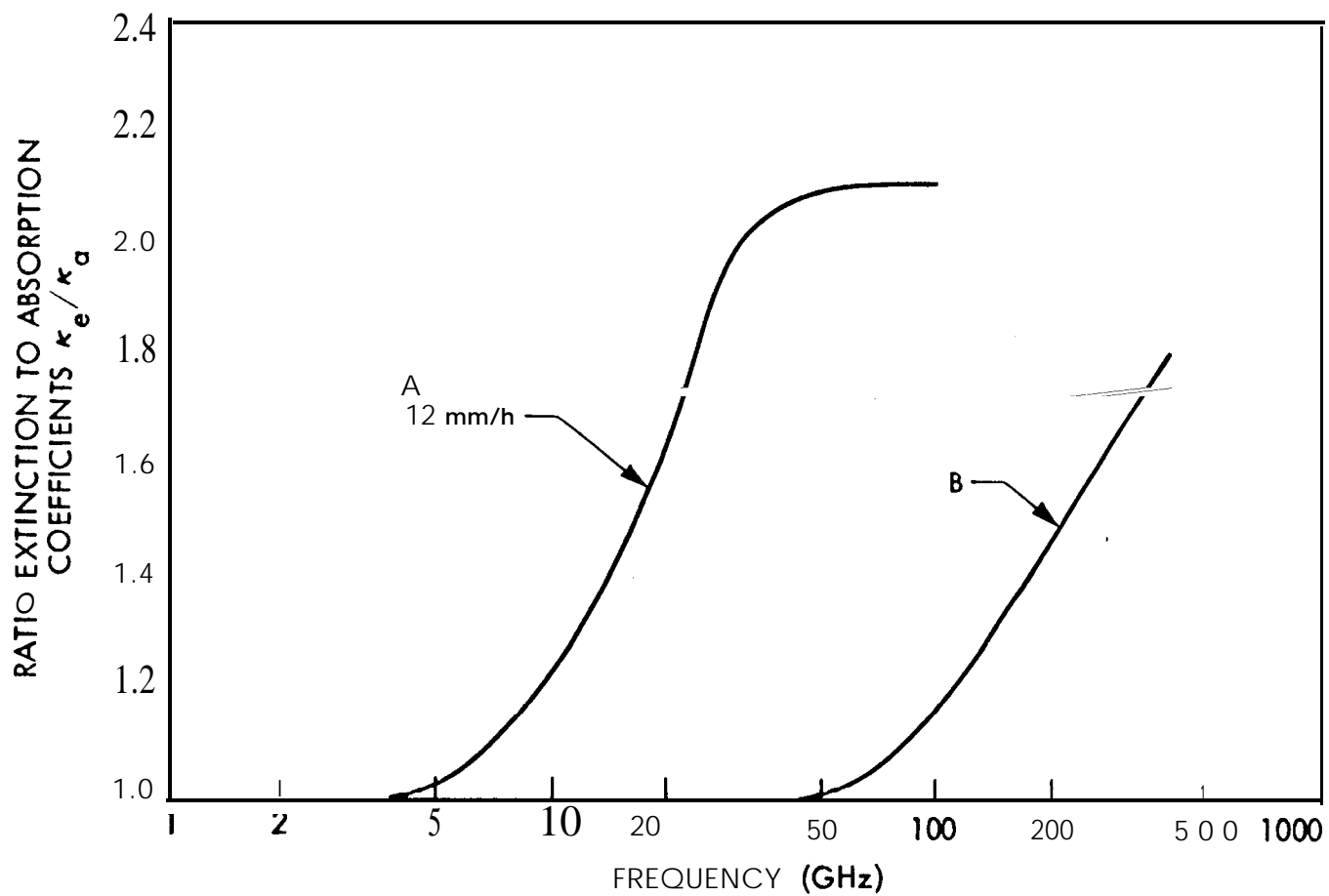


Figure 7.4. Ratio of extinction to absorption coefficients for a rain model (A) and a cloud model (B) (CCIR, 1981).

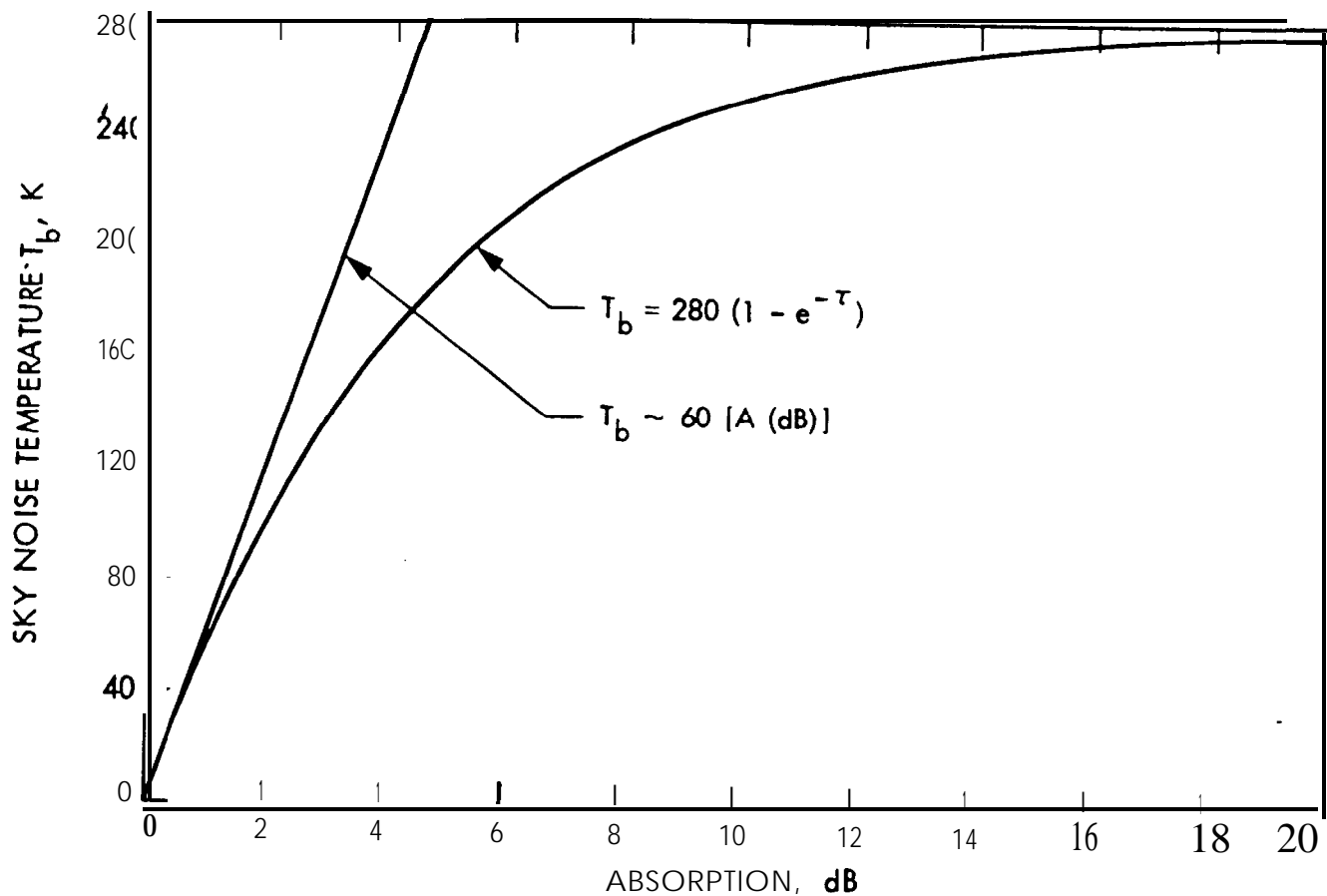


Figure 7.5. Sky noise temperature  $T_b$  due to absorbing region, assuming  $T_i = 280$  K (CCIR, 1981).

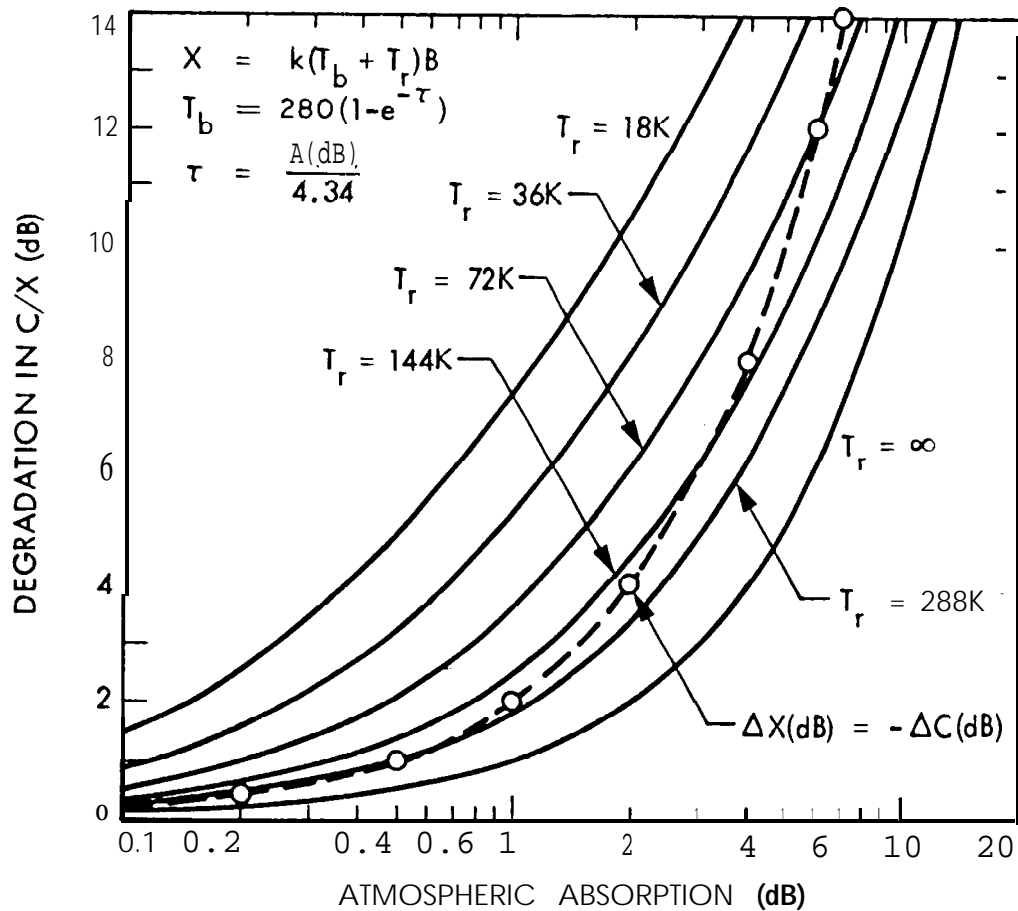


Figure 7.6. Degradation in signal-to-noise ratio,  $C/X$ , versus atmospheric absorption, for various values of  $T_1$  (taking  $T_1$  as equal to  $T_r$ ).

that the signal power  $C$  is reduced by the factor of  $e^{-\tau}$  by the rain or other source of attenuation that is being considered. The noise power  $X$  will be increased at the same time from  $X_1 = kT_1B$  to  $X_2 = kT_2B$  because of the same absorbing region. The noise power  $X_2$  is related to  $T_1$ ,  $T_2$ , and  $T_b$  of Eq. (7.23) by

$$X_2 = k (T_b + T_1) B = kT_2B \quad (7.24)$$

The optical depth  $\tau$  is related to attenuation  $A$  in dB by

$$\tau = A_{\text{dB}}/4.34 \quad (7.25)$$

where  $4.34 = 10 \log_{10} e$ . Using the above relations it develops that

$$A(C/X)_{\text{dB}} = \Delta A_{\text{dB}} + 10 \log (T_2/T_1) \quad (7.26)$$

where  $\Delta(C/X)_{\text{dB}}$  is the value of the decrease in  $C/X$ .

The dotted line in Fig. 7.6 divides the figure into two regions. To the left and above this line, the decrease in  $C/X$  due to the increase in noise is greater than the decrease  $\Delta A_{\text{dB}}$  due to attenuation. The reverse is true to the right and below the line. For example, if  $T_1 = T_R = 18$  K as may occur in the NASA-JPL Deep Space Network, absorption of 1 dB will result in an increase of noise power of about 6.5 dB and a total decrease of  $C/X$  of 7.5 dB. For large earth stations of the type used for some satellite communications,  $T_1$  may be between 50 and 100 K, for which a 1 dB increase in absorption will result in a 2 to 3.3 dB increase in noise and a 3 to 4.3 decrease in  $C/X$ .

Attenuation due to gases of the troposphere was illustrated in Sec. 3.6, and attenuation caused by rain was discussed in Chap. 4. Some values of attenuation and noise due to clouds were given in Sec. 5.1.3, and a more extensive set of such values is given in Table 7.1 (Slobin, 1981, 1982). For low noise systems, especially for frequencies above about 10 GHz but also for frequencies as low as 8.5 GHz, clouds are an important source of noise. The values of Table 7.1 apply for zenith paths (elevation angle of 90 deg). Attenuation for elevation angles  $\theta$  less than 90 deg but greater than 10 deg can be obtained from

$$A(\theta) = A_{\text{zenith}}/\sin \theta \quad \text{dB} \quad (7.27)$$

TABLE 7.1 Sample Cloud Models and S-, X-, KA-Band Zenith Effects (Slobin, 1981, 1982).

Case	Lower Cloud		Upper Cloud		Remarks	S-Band (2.3 GHz)		X-Band (8.5 GHz)		X-Band (10 GHz)	
	Density g/m <sup>3</sup>	Thick- ness km	Density g/m <sup>3</sup>	Thick- ness km		T(K)	A(dB)	T(K)	A(dB)	T(K)	A(dB)
1					Clear Afr	2.15	.035	2.78	0.45	3.05	.049
2	0.2	1.0 1.2	0.2	0.2	Thfn Cl ouds	2.16	.036	2.90	.047	3.22	.052
3			0.2	0.2		<b>2.16</b>	<b>.036</b>	2.94	<b>.048</b>	<b>3.28</b>	<b>.053</b>
4	0.5	1.0 1.5	0.5			2.20	.036	3.55	<b>.057</b>	<b>4.12</b>	<b>.066</b>
5			0.5	0.5		2.22	.037	3.83	<b>.062</b>	<b>4.50</b>	<b>.073</b>
6	0.5	1.0 2.0	1.0		<b>Medium</b> Cl ouds	2.27	.037	4.38	<b>.070</b>	<b>5.27</b>	<b>.084</b>
7			0.5	1.0		2.31	.038	4.96	<b>.081</b>	<b>6.06</b>	<b>.098</b>
8	0.5	1.0 2.0	1.0	1.0	Heavy Cl ouds	2.43	.040	6.55	<b>.105</b>	<b>8.25</b>	<b>.133</b>
9	0.7	1.0 2.0	1.0	1.0		2.54	.042	8.04	<b>.130</b>	<b>10.31</b>	<b>.166</b>
10	1.0	1.0 2.0	1.0	1.0		2.70	.044	10.27	<b>.166</b>	<b>13.35</b>	<b>.216</b>
11	1.0	1.0 2.5	1.5	1.5	<b>Very</b> Heavy Cl ouds	3.06	.050	14.89	<b>.245</b>	<b>19.66</b>	<b>.326</b>
12	1.0	1.0 3.0	2.0	2.0		3.47	.057	20.20	<b>.340</b>	<b>26.84</b>	<b>.457</b>

Notes:

- 1) Clear and cloud models as described in text
- 2) Cases 2-12 are clear air and clouds combined
- 3) Antenna located at sea level
- 4) Heights are above ground
- 5) No cosmic background or ground contribution considered
- 6) T(K) is atmospheric noise temperature at zenith
- 7) A(dB) is atmospheric attenuation along vertical path from ground to 30 km above ground

For lower elevation angles, the following expression has been used.

$$A(\theta) = \frac{2 A_{\text{zenith}}}{\sin^2\theta + 0.00235 + \sin \theta} \quad \text{dB} \quad (7.28)$$

Figure 7.7 shows values of noise temperature for a clear atmosphere having a water vapor density of  $7.5 \text{ g/m}^3$  (CCIR, 1986). For a zenith path ( $\theta = 90 \text{ deg}$ ), the noise values are small for frequencies of 10 GHz and lower. Note, however, that for angles of about 10 deg and less the noise temperature values tend to be significant. For  $\theta = 0 \text{ deg}$ , as for a terrestrial path, the noise temperature becomes about 140 K at 10 GHz. Atmospheric and other types of natural radio noise are treated in a mini-review by Flock and Smith (1984).

## 7.3 EXTRATERRESTRIAL NOISE

### 7.3.1 Introduction

While studying atmospheric noise from thunderstorms, Jansky, an engineer with the Bell Telephone Laboratories, first identified radio noise of extraterrestrial origin (Jansky, 1932, 1933). The identification was made while conducting direction-finding observations at a frequency of 20.5 MHz. Three sources of noise were recorded -- noise from nearby thunderstorms, noise from distant thunderstorms, and noise of cosmic or extraterrestrial origin. The cosmic noise came from a region having a right ascension angle near 18 h and a declination angle near -10 deg, which is the direction of the center of the Galaxy. Jansky noted that the extraterrestrial noise was often the limiting factor with respect to the detection of weak signals in the frequency range he was working in.

Reber followed up on Jansky's work by constructing and operating a receiving system having a 9.5 m paraboloidal reflector in his backyard in Wheaton, Illinois. Utilizing a frequency of 160 MHz, he constructed the first radio map of the Milky Way (Reber, 1940). Later he investigated the intensity distribution of cosmic noise at 480 MHz (Reber, 1948).

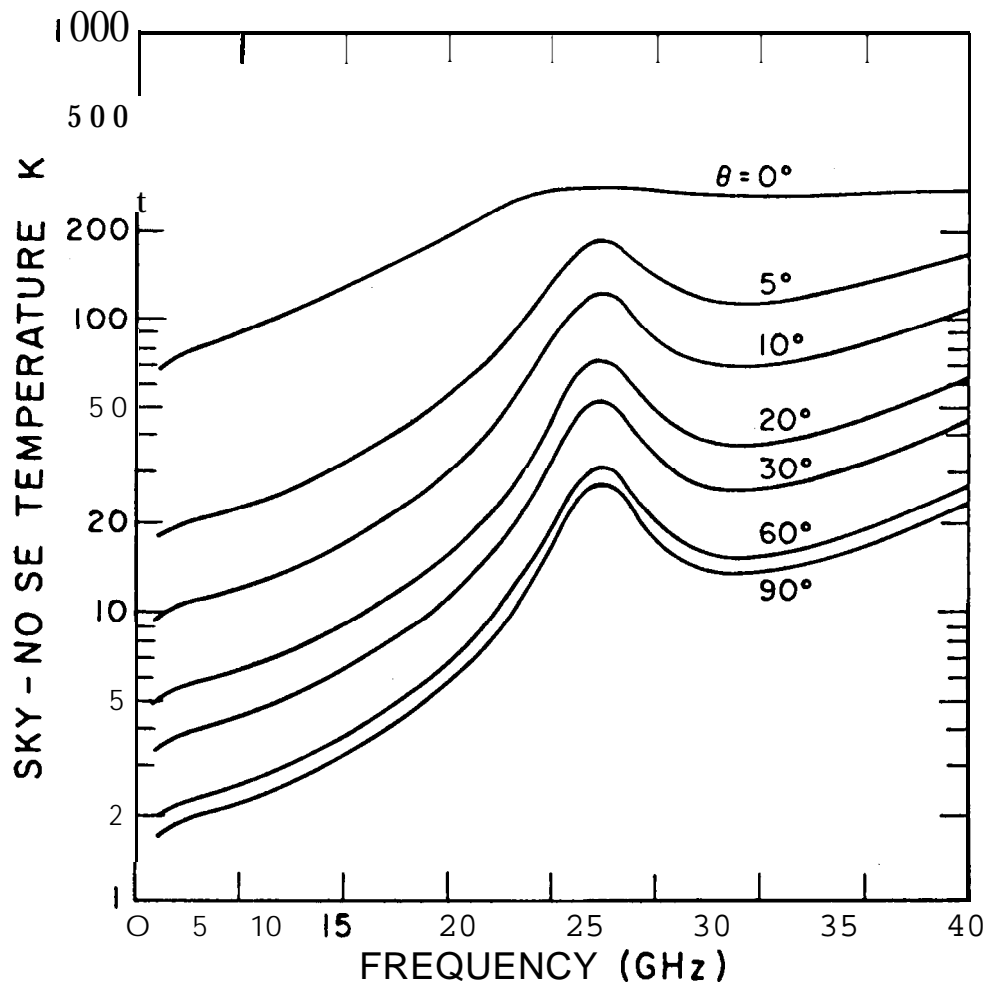


Figure 7.7. Sky-noise temperature for a water vapor density of  $7.5 \text{ g/m}^3$  as a function of elevation angle  $\theta$  (CCIR, 1 986).

The first recorded recognition of radio emission from the Sun was made in 1942 by Hey (1946), who was concerned with radio noise causing interference to 5-m radars in southern England during World War II. Jamming by German forces was suspected at first in a particular case in February 1942, but it was concluded that the noise was associated with a large sunspot. Later in the same year, Southworth (1945) of the Bell Telephone Laboratories observed thermal emission from the quiet Sun at centimeter wavelengths. Reber (~ 1944) did not succeed in detecting the Sun by radio means until 1943-1944, as at frequencies of a few hundreds of MHz the Milky Way appears brighter than the Sun when viewed with a broad-beam antenna at radio frequencies.

The first observation of emission from a discrete radio source other than the Sun, namely from Cygnus A, was made by Hey, Parsons, and Phillips (1946). The identification as a discrete source was originally made for the wrong reason. Emission from the source was thought to vary in amplitude as mentioned when introducing the subject of ionospheric scintillation (Sec. 2.6.1). Observations by Bolton and Stanley (1948), utilizing the resolution obtained by interference between direct and reflected rays at a location on a cliff overlooking the sea, however, showed that the source was indeed discrete, in fact confined to 8 min of arc. Their observations were made mainly at 100 MHz, for which they reported that the source had an effective temperature of  $4 \times 10^6$  K. In the same year, Ryle and Smith (1948), utilizing a frequency of 80 MHz, identified another strong discrete radio source, Cassiopeia A.

The brightness of the sky at radio frequencies does not correspond to that at optical frequencies, and it has been difficult to identify radio sources with visible objects. The first such identification was made by Bolton, Stanley, and Slee (1949), who identified the radio source Taurus A with the Crab Nebula, the expanding shell of the supernova of 1054 A.D. The prediction in 1945 by van de Hulst of emission by neutral hydrogen at 1421 MHz (Kraus, 1966) and the subsequent detection of such emission by Ewan and Purcell (1951) at Harvard was an important development. The emission by neutral hydrogen is due to a hyperfine transition between two states corresponding to the electron spin being parallel



or antiparallel to the spin of the nucleus (the proton). The probability of spontaneous emission of this type is very low, but the extent of interstellar space is so vast that the total amount of emission by hydrogen in space is sufficient to be observable in our galaxy and also in nearby galaxies.

Since the early developments mentioned above many discrete sources of radio emission have been identified and much progress has been made in mapping and cataloging both discrete sources and background radiation. Interesting histories of the radio observations of extraterrestrial sources have been given by Shklovsky (1960) and Hey (1983), and a valuable thorough account of radio astronomy has been prepared by Kraus (1986). Radio sources are useful for calibrating radio telescopes and, in discussing this topic, Wielebinski (1976) has presented a list of radio sources. The proceedings of IAU Symposium No. 74 include reports on a number of efforts in the mapping of radio sources (Jauncey et al., 1977), and treatments of radio sources have been presented by Fomalont (1981), Kellerman and Pauliny-Toth (1981), and Miley (1981).

The discovery by Penzias and Wilson (1965) of microwave background radiation corresponding to about 3 K in temperature was an important development which earned the Nobel Prize for them (Wilson, 1979). The radiation is believed to be relic radiation from the formation of the universe. It displays a high degree of isotropy, varying by only about 0.003 K in 24 hours. Shankar and Webster (1968) analyzed the values of microwave flux at 12 different frequencies as reported by various observers. They concluded that the values were in agreement with blackbody radiation from matter at 2.68 K, and a value of 2.7 K is commonly assigned to microwave background radiation.

### 7.3.2 Thermal Emission

Radio noise may be due to thermal or non-thermal emission and may cover a continuum of frequencies or occur at a discrete line frequency. Thermal emission from blackbodies obeys the Rayleigh-Jeans law in the radio-frequency range so that the noise power  $w$  received from a uniform source is given by

$$w = (2kT/\lambda^2) \Omega_s \quad \text{W/m}^2/\text{Hz} \quad (7.29)$$

where  $k$  is Boltzmann's constant ( $1.38 \times 10^{-23}$  J/K),  $T$  is temperature in kelvins,  $\lambda$  is wavelength in m, and  $\Omega_s$  is the solid angle in steradians subtended by the source. It can be seen that  $w$  varies inversely with wavelength squared or with  $\lambda$  to the -2 power. The exponent  $n$  of  $\lambda$  is known as a spectral index (Kraus, 1966). A hot blackbody emits thermal radiation and thus tends to be a strong emitter at infrared and optical frequencies but a weak emitter at radio frequencies.

Emission from neutral hydrogen is line emission (most prominently at the discrete frequency of 1421 MHz), but emission from ionized hydrogen, such as occurs near hot stars, is a form of thermal emission. The thermal radiation comes from free electrons experiencing acceleration, as when deflected in passing near a proton. The spectral index for ionized hydrogen can range from 0 to -2. Flux from a region of ionized hydrogen is as described by Eq. (7.29) but  $T$  can be either a constant for which  $n = -2$  or can vary as wavelength squared for which  $n = 0$ . Recall that the brightness temperature  $T_b$  when viewing a region of intrinsic brightness  $T_i$  having an optical depth of  $\tau$  is given by

$$T_b = T_i(1 - e^{-\tau}) \quad (7.30)$$

For a region containing free electrons  $\tau$  is inversely proportional to frequency squared or directly proportional to wavelength squared, and for high frequencies (e.g. 3 GHz) for which  $\tau$  is very small

$$T_b \approx T_i \tau \propto T_i \lambda^2$$

Then  $T$  of Eq. (7.29) becomes  $T_b$  and is proportional to wavelength squared so that  $n = 0$ . For lower frequencies for which  $\tau$  is large  $T_b \approx T_i$ ,  $w$  varies inversely with  $\lambda^2$ , and  $n = -2$ .

### 3.3 Non-thermal Emission

The mechanism believed to be responsible for most non-thermal emission is synchrotrons radiation. This form of radiation occurs when high velocity electrons follow spiral paths in magnetic fields (Jackson, 1962; Kraus, 1986). The electrons may be cosmic ray particles having relativistic velocities. Alven and Herlofson (1950) first suggested that the intense radio emission at low frequencies is due to synchrotrons radiation. Consider a relativistic electron moving in a circular orbit. Under this condition, radiation from the electron is concentrated in a narrow cone of width  $\theta$  which is pointed in the direction of the instantaneous velocity, as suggested in Fig. 7.8. An observer in this direction will observe a short burst of linearly polarized radiation, with its electric field intensity vector oriented as shown in the illustration. Such radiation has a broad frequency spectrum. The spectral index for synchrotrons radiation derived from cosmic-ray particles tends to be around 0.75 so that the power density of the radiation,  $w$ , is proportional to  $\lambda^{0.75}$ . Note that unlike the case for thermal emission, the spectral index for non-thermal emission is positive. Table 7.2 gives flux densities  $w$  and spectral indices for certain strong discrete sources of radio noise at frequencies indicated in the table.

Line emission from neutral hydrogen is a form of nonthermal emission. It has provided a picture of the spiral structure of our galaxy. Cassiopeia A, in our galaxy, the most intense discrete source of radio noise in the sky other than the Sun is a nonthermal

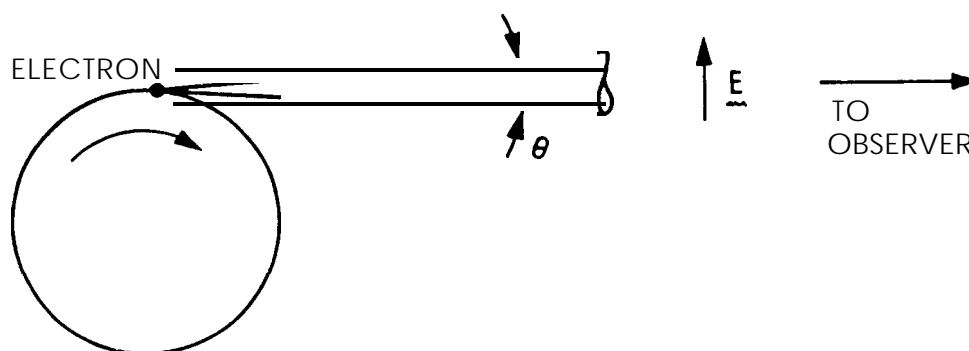


Figure 7.8. Beam of radiation from a very high velocity electron.

Table 7.2 Flux Densities and Spectral Indices for Some Nonthermal Sources (Kraus, 1986).

Source	Noise Power Density, w (Janskys) <sup>1</sup>	Frequency (MHz)	Spectral Index
Cassiopeia A	11,000	178	0.77
Cygnus A	8,700	178	≈0.6
Crab nebula	1,000	1,000	0.27
Virgo A	580		0.83
Cygnus loop	300	100	0.4 -0.5

<sup>1</sup> One Jansky (Jy) =  $10^{-26}$  W/m<sup>2</sup>/Hz.

source. Cassiopeia A is a remnant of a supernova believed to have occurred in about 1700. The crab nebula is a remnant of a supernova listed in Chinese chronicles as having occurred on July 4, 1054. The Cygnus loop is also a supernova remnant. Cygnus A, the second most intense noise source other than the Sun, is a double galaxy outside our own that has a total radio power output of  $10^{38}$  W. Virgo A is a galaxy having a radio power output of  $10^8$  W.

#### 7.3.4 The Sun, Moon, and Planets

The Sun emits as a blackbody with a temperature near 6000 K in the optical range, but at radio frequencies (below about 30 GHz) the emission from the quiet Sun is greater than that for a blackbody at this temperature and emission from the disturbed Sun is much greater yet at radio frequencies. Radiation at a particular frequency  $f$ , where  $f \approx f_p$ , comes mostly from a layer located just

above a critical layer having a plasma angular frequency  $\omega_p = 2\pi f_p$  given by

$$\omega_p^2 = \frac{Nq^2}{m\epsilon_0}$$

where  $N$  is electron density,  $q$  is electron charge,  $m$  is electron mass, and  $\epsilon_0$  is the electric permittivity of empty space (Sec. 2.1).

As  $N$  decreases with altitude, the lower frequencies are emitted from higher regions of the solar corona. The Sun appears larger and brighter at radio frequencies than for visible frequencies. The equivalent blackbody temperature for radio frequencies may be  $10^7$  K or higher (Kraus, 1986). Note that  $\omega_p$  is the same quantity that appears in  $K = 1 - \omega_p^2/\omega^2$ , where  $K = \tilde{n}$  is the relative dielectric constant for the ordinary wave in a plasma [see Eq. (2.9) 1].

Radio emission from the Sun can be classified into three components, that from the quiet Sun, a slowly varying component from bright regions, and bursts from transient disturbances such as solar flares (Kundu, 1965; Elgaroy, 1977). The slowly varying component is most prominent in the 3 to 60-cm wavelength range. Emission at 10.7 cm has been recorded for many years at Ottawa, Canada. Data from observatories recording radiation at 3, 10.7, 21, and 43 cm and 169 MHz are included in the Solar-Geophysical Data reports issued by NOAA, Boulder, Colorado. Bursts are classified into centimeter bursts, decimeter bursts, and bursts at meter and decameter wavelengths. The latter are further divided into Types I, II, III, IV, and V.

Centimeter-wave bursts have a rapid rise in intensity and a slower decline and cover essentially a smooth continuum of frequencies. The more complex decimeter bursts show a great variety of fluctuations superimposed on the continuum. Type I or noise storm radiation consists of a slowly varying, broadband enhancement of the normal solar radiation on which a series of bursts near 5 MHz are superimposed. The enhanced radiations last from hours to days, and the bursts last from a fraction of a second to several seconds. The radiation is strongly circularly polarized. Type II and III bursts are intense events whose frequencies drift lower at rates of about 1 MHz/s and 20 MHz/s respectively. Type IV bursts cover a smooth continuum of frequencies having wavelengths from centimeters to decimeters and last from about 10 minutes to a few hours. Type V bursts are also continuum events but last only for seconds to minutes and are usually limited to meter wavelengths.

When the beam of a receiving antenna comes close to the Sun, the noise due to the Sun increases in a manner dependent upon the characteristics of the antenna pattern and the relative positions of

the Sun and the antenna beam. Figure 7.9 shows the recorded increase in system noise temperature for the 64-m, S-band antenna of the Deep Space Network of the Jet Propulsion Laboratory when tracking Pioneer 8 (Nov. 1968, near the solar maximum).

Radio emission from the Moon was first detected, at a wavelength of 1.25 cm, by Dicke and Beringer (1946). The mean brightness temperature for the Moon for the S and X bands is about 240 K (JPL, 1977), and the Moon has the rather large angular size of about 0.5 deg. The observed temperature at microwave temperatures varies slightly with the phase of the Moon, reaching a maximum about 3.5 days after full moon. As for the general case, the noise temperature of an antenna that is pointed at the Moon is the average temperature for the beam. If other sources of noise can be neglected, the average temperature is about

$$240 \left( \frac{\Omega_{\text{moon}}}{\Omega_{\text{antenna}}} \right) \text{ if } \Omega_{\text{moon}} < \Omega_{\text{antenna}}$$

where  $\Omega_{\text{moon}}$  the solid angle of the Moon is  $(\pi/4)\theta_{\text{moon}}^2$ , with  $\theta_{\text{moon}}$  the angular width of the Moon, and  $\Omega_{\text{antenna}}$  is the solid angle of the antenna [as a rough rule of thumb about  $(4/3)\theta_{\text{hp}}\phi_{\text{hp}}$ , where the latter angles are half-power beamwidths].

Emission from the planets is of much interest from the viewpoint of radio science, the intense, sporadic, and fluctuating emission of Jupiter being especially noteworthy. Equation (7.30) gives the relation used by JPL (1977) for estimating the increase  $T_{\text{pi}}$  in system noise temperature due to certain planets at the S and X' bands, assuming the planets fall within the antenna beamwidth.

$$T_{\text{pi}} = \frac{S_0 \lambda^2}{8\pi k R^2} G e^{-2.77 (\theta^2/\theta_{\text{hp}}^2)} \quad (7.30)$$

In Eq. (7.30),  $S_0$  is the flux density in  $\text{W}/\text{m}^2/\text{Hz}$  at a range of 1 AU ( $1.5 \times 10^{11}$  m),  $R$  is the range of the planet in AU,  $k$  is Boltzmann's constant,  $\lambda$  is wavelength,  $G$  is antenna gain modified to include atmospheric attenuation,  $\theta$  is the planet-earth-probe angle in deg, and  $\theta_{\text{hp}}$  is the half-power beamwidth of the antenna in deg. The flux densities  $S_0$  in Janskys at 1 AU for some planets are given in Table 7.3.

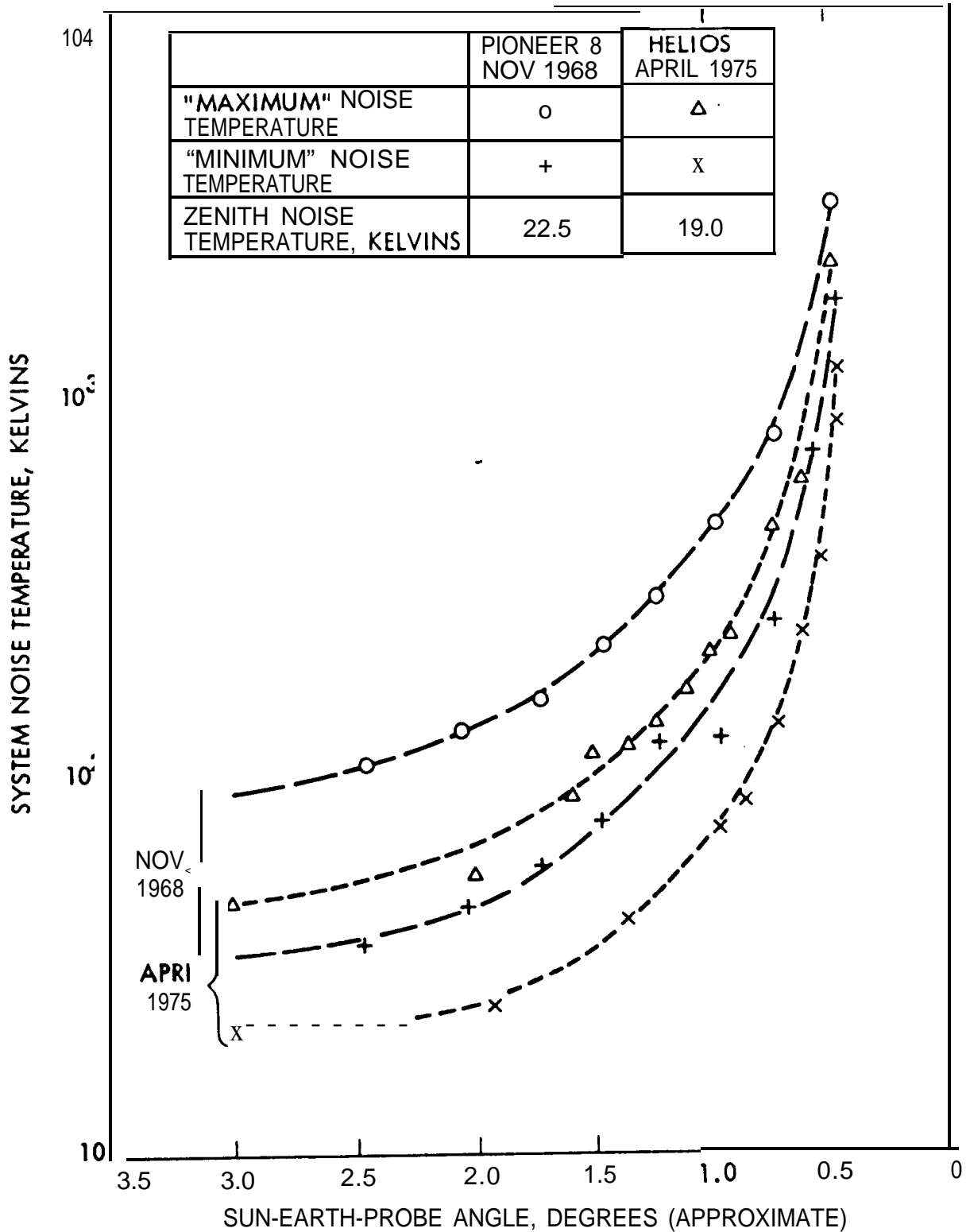


Figure 7.9. System noise temperature vs. sun-earth-probe angle at S band for 64-m antenna stations, from measured data (JPL, 1977).

Table 7.3 Flux Density  $S_0$  in Janskys (Jy) at One AU,  
 (1 Jy =  $10^{-26}$  W/m<sup>2</sup>/Hz.)

Planets	S Band	X Band
Venus	0.53	7.4
Mars	0.050	0.68
Saturn	14	170
Jupiter	91 to 118	330

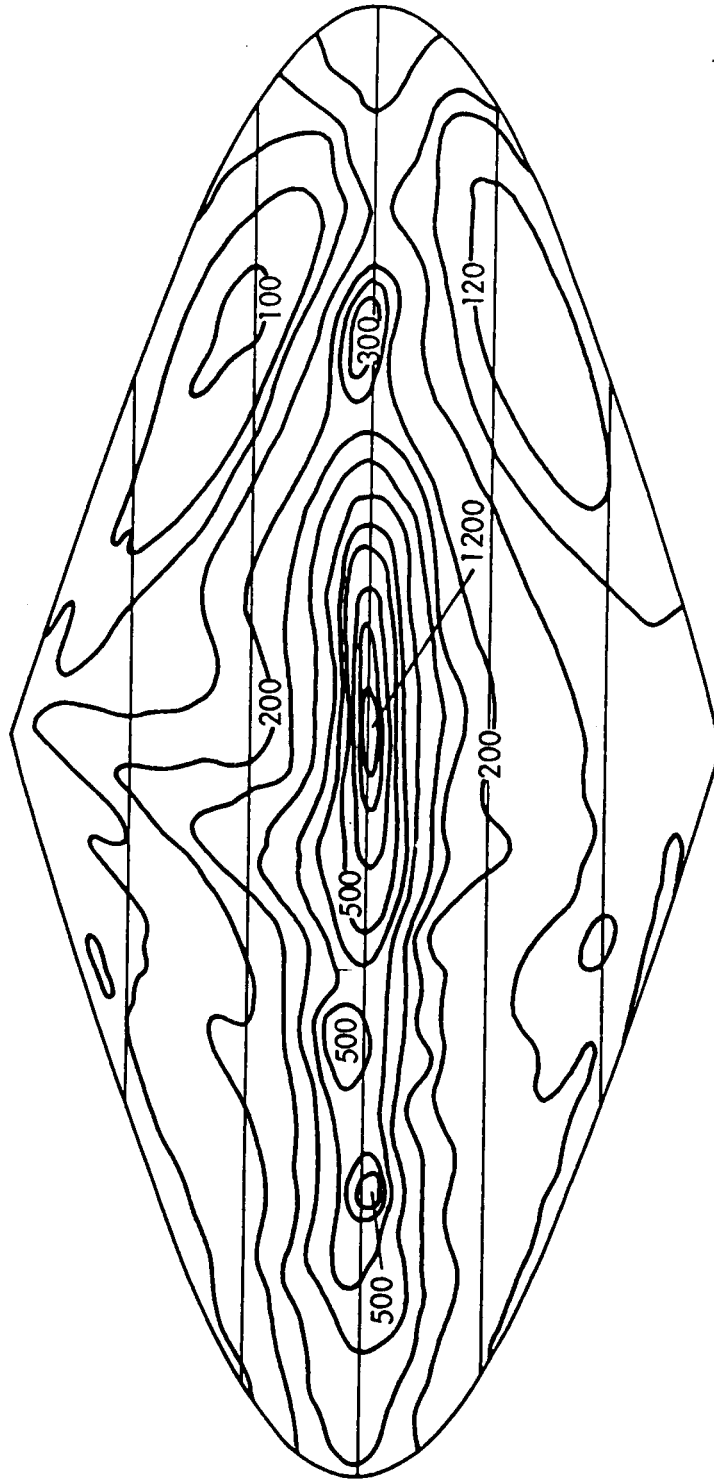
### 7.3.4 Satellite Operations

A radio map of our galaxy at a frequency of 400 MHz for a beamwidth of 1 deg is shown in Fig. 7.10. The plot is in galactic coordinates and is quite symmetrical with respect to the galactic equator. A noise temperature of 1200 K is shown for the center of the Galaxy. Figure 7.11 shows a similar plot, but for a frequency of 250 MHz and in celestial coordinates, with the zero declination angle corresponding to the Earth's equator. For geostationary satellites the corresponding values of declination  $\delta$  are restricted to about  $\pm 8.7$  deg. For an earth station at the highest possible latitude of about 81.3 deg for communicating with a geostationary satellite,  $\delta = \sin^{-1} 6356 / (35,786 + 6356) = 8.7$  deg where 6356 is the polar radius and 35,786 km is the altitude of a geostationary satellite. Haslam et al. (1982) have surveyed the radio sky at 408 MHz with an angular resolution of 0.85 deg. Plots of the results of this survey, "smoothed to 5 deg angular resolution, are included in CCIR (1986).

The contours of Fig. 7.11 are in units of 6 K above 80 K, the value of the coldest parts of the sky. For an 18 h right ascension angle and 0 deg declination, for example, the value from Fig. 7.11 is 37 and the brightness temperature is 302 K at 250 MHz. To estimate the brightness temperature at a higher frequency note that brightness  $B$  of blackbodies at radio frequencies is given by

$$B = 2kT/\lambda^2 \quad \text{W /m}^2\text{/Hz/rad}^2 \quad (7.32)$$





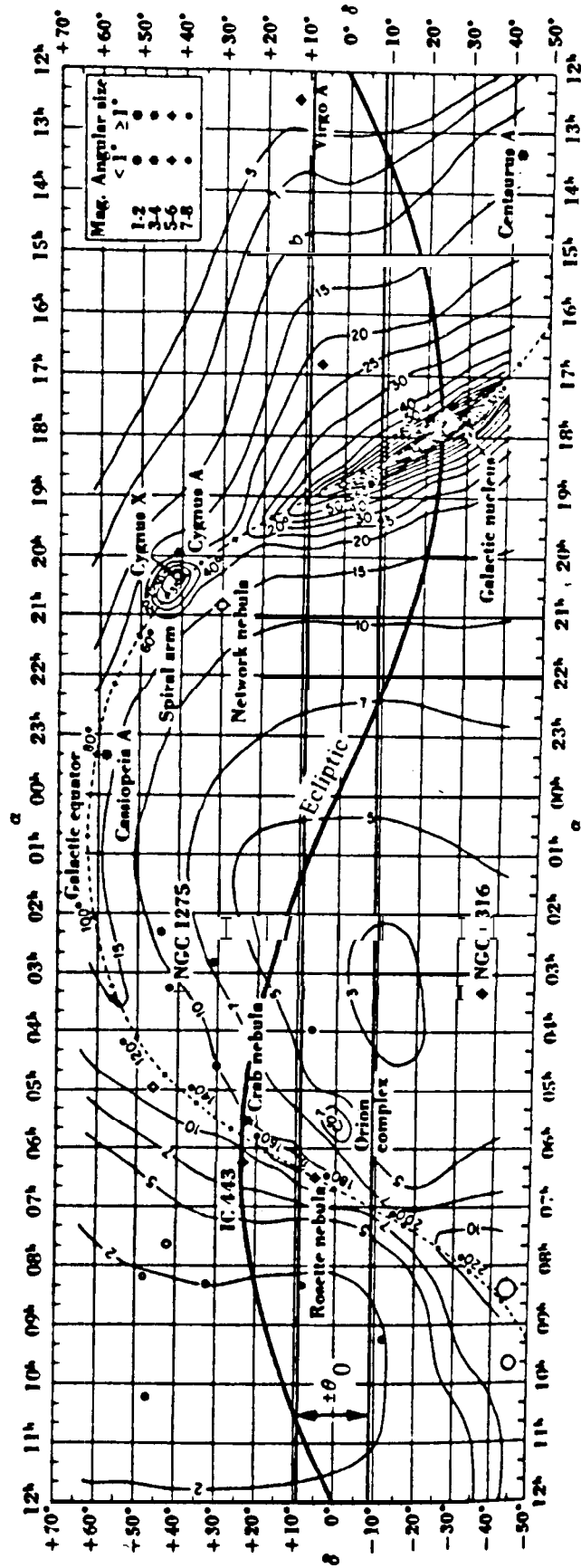
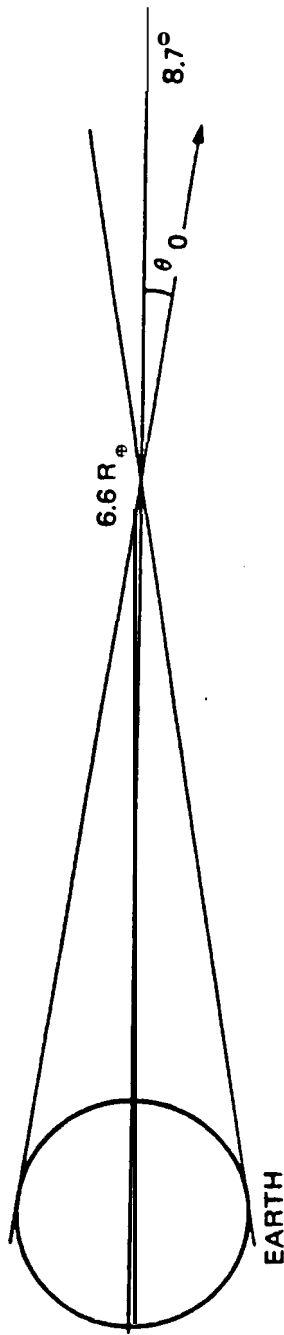


Figure 7.1 Radio sky at 250 MHz as a background for that part of the celestial sphere of interest in earth-satellite telecommunications using the geostationary orbit (CCIR, 1981; Kraus, 1966).

It can be shown that an antenna receiving radiation from a blackbody, assuming that it fills the antenna beam, will receive the power per Hz,  $w$ , given by (Flock, 1979)

$$w = kT \quad \text{W/Hz} \quad (7.33)$$

For the case of nonthermal radiation, an equivalent blackbody temperature can be assigned even though blackbody-radiation theory does not apply. If the spectral index for nonthermal radiation is 0.75 and  $T$  of Eq. (7.32) is to be defined as an equivalent blackbody brightness temperature so that the Rayleigh-Jeans law can be utilized, then  $T$  must vary as  $\lambda^{2.75}$  or  $f^{-2.75}$  (Smith, 1982a). On this basis the brightness temperature at a microwave frequency can be determined from  $T$  for 250 MHz (referred to as  $f_0$ ) by

$$T_b(f_i) = T_b(f_0) (f_i/f_0)^{-2.75} + 2.7 \quad \text{K} \quad (7.34)$$

For example, if  $f_i = 1$  GHz

$$T_b = 302 (4)^{-2.75} + 2.7 = 9.4 \text{ K}$$

while for  $f_i = 4$  GHz

$$T_b = 302 (16)^{-2.75} + 2.7 = 2.8 \text{ K}$$

The quantity 2.7 K represents the microwave background radiation investigated by Penzias and Wilson (1965), and  $T_b$  for  $f_i = 4$  GHz is close to this microwave background level. The brightness temperature  $T_b$  in the situation being considered is a strong function of frequency and decreases to a very low value in the S band.

For frequencies above 2 GHz, the extraterrestrial sources of importance are the Sun and a few non-thermal sources such as Cassiopeia A, Cygnus A and X, and the Crab Nebula (CCIR, 1986). Examination of Fig. 7.10, however, shows that the non-thermal sources mentioned are not of concern for geostationary satellites as these sources fall outside the range for  $\delta$  of  $\pm 8.7$  deg. For deep

space missions, the value of  $\delta$  can be near  $\pm 23.5$  deg, corresponding to the ecliptic, or larger and somewhat larger values of noise may be encountered than for geostationary satellites.

### 7.3.5 Quasars and Pulsars

Quasars are distant galaxies that look like stars on photographs but are characterized by very large Doppler shifts (redshifts) such that their spectra were not recognized originally. The radio source 3C 48 was first located in 1960, and it was after the discovery of a similar source 3C 273 in 1963 that the large redshifts and corresponding high receding velocities were identified by noting that the observed emission spectrum was that of hydrogen except that it was shifted in frequency by a large amount. The high velocities indicate that quasars (quasi-stellar objects) are at great distances. In order to be seen at such distances, they have to emit extremely high powers at optical frequencies. Many quasars also emit large quantities of radiation at radio frequencies,

Pulsars are considered to be rotating neutron stars which emit radio-frequency or x-ray radiation in the form of a narrow beam, so that an observer on the Earth records short pulses at a regular repetition rate. Jocelyn Bell first identified pulsar signals on Cambridge radio-telescope records of interplanetary scintillation in late 1967. Short pulses, 0.016 second in duration were observed every 1.33730115 second. In 1968 David Staelin and Edward Reifstein found a pulsar in the middle of the Crab Nebula, a remnant of the 1054 supernova. Pulse periods of most pulsars range from 0.033 to 3.7 seconds with a median value of 0.65 second (Hey, 1983). Pulse lengths are always a few percent of the corresponding pulse periods.

The discoveries of quasars and pulsars were extremely exciting to radio astronomers, and both quasars and pulsars are of great scientific interest. They are mentioned here because they contribute to radio noise. The quasars 3C 273, mentioned above, and 3C 279 occur within the  $\pm 8.7$  deg range of declination of most importance to satellite communications (Wielebinski, 1976). Quasars, pulsars, and related phenomena are treated in texts on astronomy (e.g. Abell, 1982) and in a number of more specialized publications of both a semipopular and more strictly scientific nature (Shipman, 1980; Hey, 1983).

## 7.4 NOISE OF TERRESTRIAL ORIGIN

The receiving antenna of an uplink to a satellite points at the Earth and for that reason is commonly assumed to have a noise temperature of 250 to 290 K. Actually the noise temperature is generally lower and is not determined entirely by the Earth alone. To consider the situation further refer to Fig. 7.12 and Eq. (7.35).

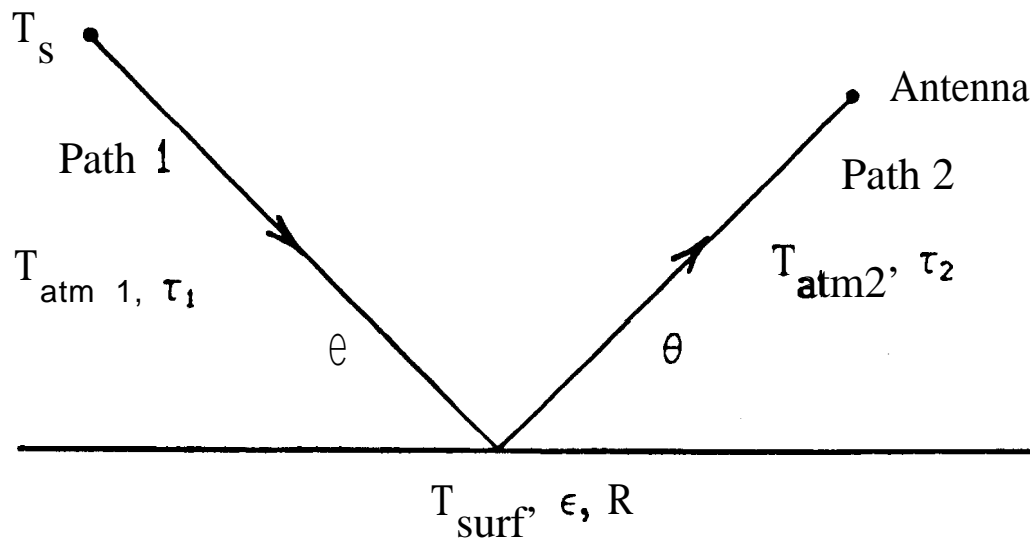


Figure 7.12. Contributions to the brightness temperature  $T_{b2}$  recorded by a downward-pointing satellite or radiometer antenna (CCIR, 1986).

The brightness temperature  $T_{b2}$  recorded by the downward pointing antenna of Fig. 7.12 has the form of

$$T_{b2} = T_{atm2} + (\epsilon T_{surf} + R T_{b1}) e^{-\tau_0} \quad (7.35)$$

where  $T_{atm2}$  accounts for the emission from the atmosphere along path 2,  $T_{surf}$  is the actual surface temperature, and  $T_{b1}$  is the brightness temperature observed when looking from the ground along path 1. The quantity  $\epsilon$  is the emissivity of the surface, and  $R$ , the power reflection coefficient for radiation incident on the surface, equals  $\rho$  squared where  $\rho$  is the appropriate reflection coefficient for horizontal, vertical, or circular polarization, etc. of Chap. 6

[Eqs. (6. 14), (6. 15), (6. 18, 6. 19)]. The optical depth  $\tau_0$  applies to path 2, from the Earth's surface to the receiving antenna.

Kirchoff's law of radiation theory states that the emissivity  $\epsilon$  of a surface is equal to its absorptivity  $\alpha$ . Both quantities have maximum values of unity. The quantity  $\epsilon$  represents the fraction of the potential blackbody radiation that is emitted, and  $\alpha$  represents the fraction of the incident radiation that is absorbed. For radiation incident upon a surface, the fraction  $\alpha$  is absorbed and the fraction  $R$  is reflected, where  $R$  is the power reflection coefficient. Thus  $\alpha + R = 1$ , and since  $|\alpha| = |\epsilon|$

$$\epsilon + R = 1 \quad (7.36)$$

We deal here with the general case of paths at any elevation angle  $\theta$ , whereas Eq. (7.21) applies to a zenith path, but otherwise  $T_{b1}$  has the form of Eq. (7.21), which is commonly written in the simpler manner of Eq. (7.22). In the present case

$$T_{b1} = T_s e^{-\tau_\infty} + T_{atm1} = T_s e^{-\tau_\infty} + \int_0^\infty T(r) \alpha(r) e^{-\tau_1(r)} dr \quad (7.37)$$

where the surface is located at  $r = 0$ ,  $h = 0$  with  $r$  the distance along path 1 and  $h$  the height.  $T_{atm1}$  accounts for atmospheric emission along path 1. Similarly

$$T_{atm2} = \int_0^{\text{antenna}} T(r) \alpha(r) e^{-\tau_2(r)} dr \quad (7.38)$$

In Eqs. (7.37) and (7.38)

$$\tau_\infty = \int_0^\infty \alpha(r') dr' \quad (7.39)$$

$$\tau_1(r) = \int_0^r \alpha(r') dr' \quad (7.40)$$

$$\tau_2(r) = \int_r^{\text{antenna}} \alpha(r') dr' \quad (7.41)$$

$$\tau_0 = \int_0^{\text{antenna}} \alpha(r') dr' \quad (7.42)$$

In the limited frequency range between about 3 to 10 GHz for which atmospheric absorption and emission and extraterrestrial noise may not be significant

$$T_{b2} \approx \epsilon T_{\text{surf}} \quad (7.43)$$

A similar relation is sometimes shown with a term  $R T_s$  added. Note that  $\epsilon = 1 - R = 1 - \rho^2$  and that  $\epsilon$  therefore depends on wave polarization, elevation angle, the dielectric constant and conductivity of the surface, and surface roughness, as the field intensity reflection coefficient  $\rho$  was shown in Chap. 6 to depend on these quantities. For the case of sea water,  $\rho$  and  $\epsilon$  depend on salinity and temperature. The brightness temperature at normal incidence on sea water is shown in Fig. 7.13 as a function of salinity and temperature.

Although  $T_{b2}$  is merely noise when telecommunications are being considered, it can be employed to obtain data on phenomena such as sea-surface temperature, for example. Also sea ice and sea water can be distinguished by the higher-brightness temperature of sea ice (235 to 240 K for first-year ice and about 210 to 230 K for multiyear ice). Multifrequency radiometry is needed to remove atmospheric and surface roughness effects in order to obtain sea-surface temperature in the general case, and a number of Scanning Multifrequency Microwave Radiometers (SMMR's) have been flown on various missions, the more recent ones on Seasat and Nimbus-7 having frequencies of 6.63, 10.69, 18.0, 21.0, and 37.0 GHz. The microwave radiometers compete with infrared radiometers which have greater spatial resolution and sensitivity but are limited by clouds. Another difference is that emissivity is higher and less variable with sea state and elevation angle at infrared frequencies.

Njoku and Smith (1985) have computed the microwave antenna temperature of the Earth as seen from the geostationary orbit as a function of longitude and frequency. Values ranging from 60 to 240 K have been found. They used an average surface temperature of 292 K and an emissivity of 0.93 for land resulting in a brightness temperature of 272 K for land. A cloud cover of 50 percent with 2.5 g/cm<sup>2</sup> of water vapor was assumed. Brightness temperatures of water are considerably lower than those of land as shown in Fig. 7.14. The brightness temperature at geostationary orbit depends on the fraction of the antenna beam filled by land and the fraction filled by water. The lowest land fraction 0.17 at 160 deg W and the

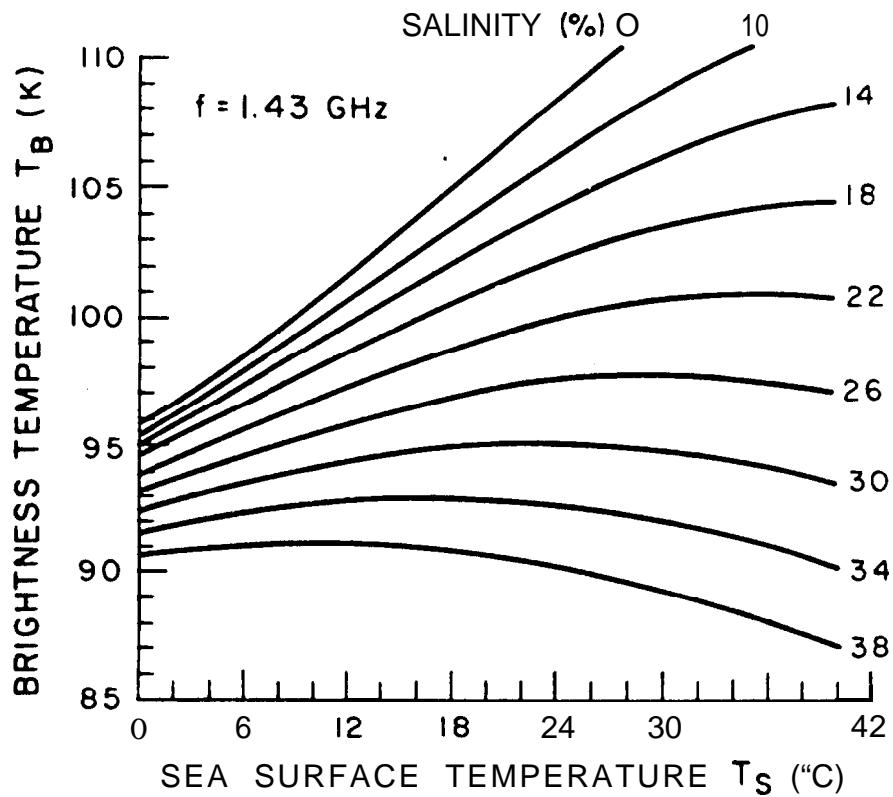


Figure 7.13. Brightness temperature at normal incidence as a function of surface temperature and salinity at a frequency of 1.43 GHz, after Swift (1980).



highest, 0.46 at 30 deg E, correspond to the lowest and highest" brightness temperatures, respectively. It is stated that a value of antenna temperature as low as 60 K at 1 GHz can result from antenna efficiencies of around 0.5 to 0.6. The efficiency affects signal intensity as well as noise and is said to not result in a decrease of signal-to-noise ratio, but the true value of antenna temperature should nevertheless be recognized. Antenna temperatures as seen from the geostationary orbit are shown in Fig. 7.14. Note that whereas Fig. 7.12 applies to the case of narrow antenna beamwidths for which a specific elevation angle can be defined, the calculation of brightness temperature from the geostationary orbit assumed that the Earth filled the antenna beam and involved determining resulting average brightness temperatures.

For the case of a downlink from a satellite, the sidelobes and backlobe of the earth-station receiving antenna pick up small amounts of radiation from the Earth. Thus the Earth provides at least a slight contribution to the noise temperature of even a high-quality earth-station antenna. The magnitude of the contribution must usually be determined empirically. Any object in the field of view of an antenna contributes to antenna noise temperature unless it is a perfect conductor. In determining the level of microwave background radiation, Penzias and Wilson (1965) found in a particular case an antenna temperature of 6.7 K when the antenna was pointed to the zenith, of which 2.7 K was cosmic relict radiation, 2.3 K was of atmospheric origin, and 0.9 K was judged to be due to ohmic losses in the antenna and back-lobe response. The latter value is for a very high-efficiency horn antenna and can be considered to be an absolute minimum value.

Noise of terrestrial origin may be natural or man-made. Consideration of man-made radio noise is outside the scope of this handbook. A useful treatment has been provided by Skomal (1978). Chapters are included in his text about noise from automobiles, electric-power systems, and industrial, scientific, and medical sources. Data on man-made noise in the 300 kHz to 250 MHz range are included in CCIR Report 258 (Volume VI, Propagation in Ionized Media), and maximum and minimum levels of radio noise, including man-made noise, are given in CCIR Report 670 (Volume I, Spectrum Utilization and Monitoring).

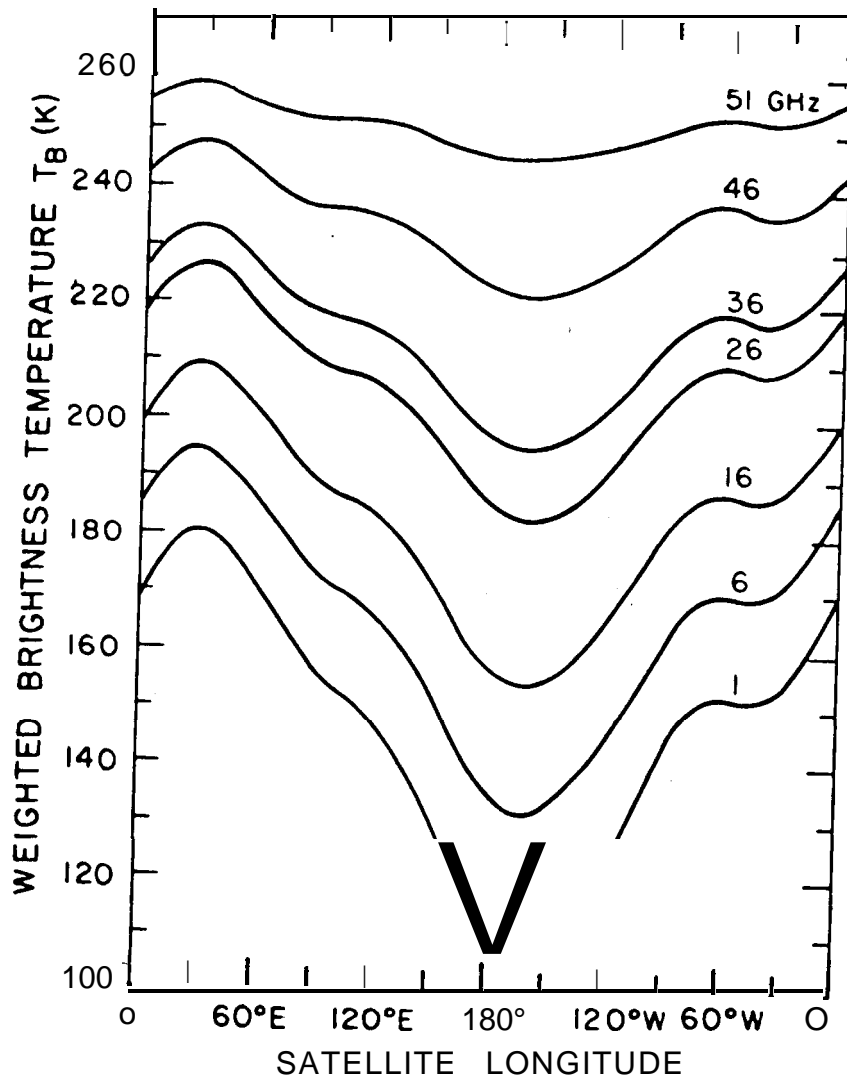


Figure 7.14. Brightness temperature of the Earth as a function of longitude as viewed from the geostationary orbit at frequencies between 1 and 51 GHz. The curves apply to the U.S. Standard Atmosphere, with a columnar content of 2.5 grams/cm<sup>2</sup> of water vapor and 50 percent cloud cover. The normalized earth-coverage antenna pattern is given by  $G(\theta) = -3 (6/8.7 - 15)\theta^2$  dB for  $0 \leq \theta \leq 8.175$  deg where  $\theta$  is the angle off boresight (Njoku and Smith, 1985).

## REFERENCES

- Abell, G. O., Exploration of the Universe. Philadelphia: CBS College Publishing, Saunders College Publishing, 1982.
- Alfven, H. and N. Herlofson, "Cosmic radiation and radio stars," *Phys. Rev.*, vol. 78, p. 616, 1950.
- Bolton, J.G. and G.J. Stanley, "Variable source of radio frequency radiation in the constellation of Cygnus," *Nature*, vol. 161, pp. 312-313, Feb. 28, 1948.
- Bolton, J. G., G.J. Stanley, and O.B. Slee, "Positions of three discrete sources of galactic radio-frequency radiation," *Nature*, vol. 164, pp. 101-102, July 16, 1949.
- CCIR, Draft Revision of Report 564-~ (Mod. 1 ), CCIR Study Group 5 Document 5/34, April 9, 1981,
- CCIR, "Radio emission from natural sources above about 50 MHz," Report 720-2, Vol. V, Propagation in Non-ionized Media, Recommendations and Reports of the CCIR, 1986. Geneva: Int. Telecomm. Union, 1986.
- Dicke, R.H. and R. Beringer, "Microwave radiation from the Sun and Moon," *Astrophys. J.*, vol. 103, p. 375, 1946.
- Droge, F. and W. Priester, "Durchmusterung der allgemeinen radiofrequenz-strahlung bei 200 MHz," *Z. Astrophys.*, vol. 40, pp. 236-248, 1956.
- Elgaroy, E. O., Solar Noise Storms. Oxford, New York: Pergamon Press, 1977.
- Ewen, H. I. and E.M. Purcell, "Radiation from galactic hydrogen at 1420 Mc/s," *Nature*, vol. 168, pp. 356-357, Sept. 1, 1951.
- Flock, W.L., Electromagnetic and the Environment: Remote Sensing and Telecommunications. Englewood Cliff, NJ: Prentice-Hall, 1979.
- Flock, W.L. and E.K. Smith, "Natural radio noise -- a mini-review," *IEEE Trans. Antennas Propagat.*, vol. AP-32, pp. 762-767, July 1984.
- Fomalont, E. B., "Extended radio sources," in *Origin of Cosmic Rays*, IAU Symposium No. 94, Setti, G. et al. (eds.), pp. 111-128. Dordrecht, Netherlands: D. Reidel, 1981.

- Haslam, C.G.T. et al., "A 408 MHz all-sky continuum survey. II. The atlas of contour maps." *Astron. Astrophys. Supp.*, vol. 47, pp. 1-143, Jan. 1982.
- Hey, J. S., "Solar radiations in the 4 to 6 meter radio wavelength band," *Nature*, vol. 157, p.47, 1946.
- Hey, J. S., The Radio Universe, 3rd Ed. Oxford, New York: Pergamon Press, 1983.
- Hey, J.S., S.J. Parsons, and J.W. Phillips, "Fluctuations in cosmic radiation at radio frequencies," *Nature*, vol. 158, p, 234, Aug. 17.1946.
- Jackson, J. D., Classical Electrodynamics, 2nd Ed. New York: Wiley, 1975.
- Jansky, K. G., "Directional studies of atmospheric disturbances at high frequencies," *Pmt. IRE*, vol. 20, pp. 1920-1932, Dec. 1932.
- Jansky, K. G., "Electrical disturbances apparently of extraterrestrial origin," *Proc. IRE*, vol. 21, pp. 1387-1398, Oct. 1933.
- Jauncey, D.L. (Ed.), Radio Astronomy and Cosmology. IAU Symposium No. 74, Dordrecht, Netherlands: D. Reidel, 1977.
- JPL, Deep Space Network/Flight Project Interface Design Handbook, Document 810-5, Rev. D, Sec. TC1 -40, DSN Telecommunication Interfaces, Atmospheric and Environmental Effects, Jet Propulsion Laboratory, Pasadena, Ca, 15 Dec. 1977.
- Kellerman, K.I. and I.I.K. Pauliny-Toth, "Compact radio sources," in *Annual Rev. Astron. Astmphys*, vol. 19, pp.373-4 10. Palo Alto, CA: Annual Reviews, 1981.
- Kraus, J. D., Radio Astronomy, 2nd edition. Powell, Ohio 43065: Cygnus-Quasar Books, 1986. (The first edition of 1966 was also useful in the preparation of this chapter.)
- Kundu, M. R., Solar Radio Astronomy. New York: Interscience Pub., 1965.
- Miley, G., "The structure of extended extragalactic radio sources," in *Annual Rev. Astron. Astrop hys.*, vol. 18, pp. 165-218. Palo Alto, CA: Annual Reviews, 1981.
- Njoko, E.G. and E. K. Smith, "Microwave antenna temperature of the earth from geostationary orbit," *Radio Sci.*, vol. 20, pp. 591-599. May-June 1985.
- Penzias, A.A. and R. W. Wilson, "A measurement of excess antenna temperature at 4080 Me/s," *Astrophys. J.*, vol. 142, pp. 419-421, 1965.

- Reber, G., "Cosmic static," Proc IRE, vol. 142, pp. 68-70, Feb. 1940.
- Reber, G., "Cosmic static," Astrophys. J. vol. 100, pp. 279-287. Nov. 1944.
- Reber, G., "Cosmic static," Proc. IRE, vol. 36, pp. 1215-1218, Oct. 1948.
- Ryle, M. and F.G. Smith, "A new intense source of radio-frequency radiation in the constellation of Cassiopeia," Nature, vol. 162, pp. 462-463, Sept. 18, 1948,
- Shakeshaft, J.R. and A.S. Webster, "Microwave background in a steady state universe," Nature, vol. 217, pp. 339,340, Jan. 27, 1968.
- Shipman, H. L., Black Holes, Quasars, and the Universe, 2nd Ed. Boston: Houghton Mifflin, 1980.
- Shklovsky, I. S., Cosmic Radio Waves, English translation by R.B. Rodman and C.M. Varsavsky. Cambridge, MA: Harvard U. Press, 1960.
- Skomal, E. N., Man-Made Radio Noise. New York: Van Nostrand, 1978.
- Slobin, S. D., Microwave Noise Temperature and Attenuation of Clouds at Frequencies Below 50 GHz, JPL Publication 81-46, Pasadena, CA: Jet Propulsion Lab., 1981.
- Slobin, S. D., "Microwave noise temperature and attenuation of clouds: statistics of these effects at various sites in the United States, Alaska, and Hawaii," Radio Sci., vol. 17, pp. 1443-1454, Nov.-Dec. 1982.
- Smith, E. K., "The natural radio noise source environment," Proc. of 1982 IEEE Int. Sym. on Electromagnetic Compatibility, Santa Clara, CA (Sept. 6-8, 1982). New York: IEEE, 1982a.
- Smith, E. K., "centimeter and millimeter wave attenuation and brightness temperature due to atmospheric oxygen and water vapor," Radio Sci., vol. 17, pp. 1455-1464, Nov.-Dec. 1982b.
- Southworth, G. D., "Microwave radiation from the sun," J. Franklin Inst., vol. 239, p. 285, 1945.
- Swift, C. T., "Passive remote sensing of the ocean - a review," Bound. Layer Meteorol., vol. 18, pp. 25-54, 1980.